Articles

Novel Self-Assembled Metallo-Homopolymers and Metallo-*alt*-copolymer Containing Terpyridyl Zinc(II) Moieties

Yi-Yu Chen,[†] Yu-Tai Tao,[‡] and Hong-Cheu Lin*,[†]

Department of Materials Science and Engineering, National Chiao Tung University, Hsinchu, Taiwan (ROC), and Institute of Chemistry, Academia Sinica, Taipei, Taiwan (ROC)

Received August 14, 2006; Revised Manuscript Received September 28, 2006

ABSTRACT: A series of novel terpyridyl Zn(II))-based metallo-polymers, including metallo-homopolymers and metallo-*alt*-copolymer, containing carbazole pendants attached to the C-9 position of fluorene by long alkyl spacers were constructed by self-assembled reaction. The integrated ratios of ^{1}H NMR reveal a facile result to distinguish the differences between metallo-homopolymers and copolymers. To further investigate these polymers, UV−vis and PL spectral titration experiments were also carried out by varying the molar ratios of zinc(II) ions to monomers. The photophysical properties of these polymers exhibited blue PL emissions (around 420 nm) with quantum yields of 11−23% (in DMF) and the PL results revealed that the formation of excimers were suppressed by the incorporation of carbazole pendant groups. In addition, the EL results showed green EL emissions (around 550 nm) with turn-on voltages of 6.0−6.5 V, maximum efficiencies of 0.85−1.1 cd A^{-1} (at 100 mA cm^{-2}), and maximum luminances of 1704−2819 cd/m^2 (around 15 V), correspondingly.

Introduction

Metal−ligand coordination seems to be particularly attractive in past few decades because of searching for new smart materials.[1−5] Moreover, by proper selections of metal−ligand combinations; it is possible to realize ideal conditions for self-assembly, i.e., formation of kinetically labile but nevertheless thermodynamically stable bonds. The properties of coordination polymers can be widely varied due to the availability of a multitude of ions and ligands, both having profound effects on binding strength, reversibility, and solubility.[6] Accordingly, it is not surprising that metal−ligand coordination polymers, which are processable in solutions, have gained considerable interest in recent years.

2,2′:6′,2″-Terpyridine is one of the metal−ligand combination units that have been of particular importance for construction of metallo-supramolecular polymers,[5,7] and a large number of studies have been reported on the construction of linear-rod polymers based on this terpyridyl unit.[8] Due to the prominent photoluminescent (PL) and electroluminescent (EL) properties, terpyridyl Zn(II) moieties were introduced to optoelectronic applications by several research groups.[5,9] During the process of light emission in the fully conjugated metallo-polymers, it is confirmed that the phenomenon of metal to ligand charge transfer (MLCT) does not occur in terpyridyl Zn(II) moieties because of the d^{10} Zn(II) species, so only intraligand charge transfer (ILCT) happens between the coordination sites and chromophores.[10] Dobrawa and Würthner have recently reported

that metallo-polymers containing perylene bisimide dyes and terpyridyl Zn(II) moieties showed strong red PL emissions.[10a−b] According to Che and co-workers' report, the incorporation of terpyridyl Zn(II) moieties into different main-chain structures was proven to exhibit different emission wavelength ranging from violet to yellow colors with high PL quantum yields, and the applications of high efficient polymeric light-emitting diode (PLED) devices are plausible by using these coordination polymers.[11] Therefore, utilization of terpyridyl Zn(II) moieties as connecting groups to assemble suitable chromophores is an appealing strategy for the construction of PL or EL metallo-supramolecular polymers. In this study, novel terpyridyl Zn(II)-based metallo-polymers, including metallo-homopolymers and metallo-*alternating*-copolymer (i.e., metallo-*alt*-copolymer), containing carbazole pendants attached to the C-9 position of fluorenes by long alkyl spacers were constructed by self-assembled reaction and their ^{1}H NMR, PL, and EL properties were investigated as well. More importantly, the first light emitting metallo-*alt*-copolymer built up from different ditopic ligands coordinating with Zn(II) species was developed and is surveyed in this report.

Experimental Section

Measurements. ^{1}H NMR spectra were recorded on a Varian Unity 300 MHz spectrometer using CDCl$_3$ and DMSO-d_6 solvents. Elemental analyses were performed on a HERAEUS CHN−OS RAPID elemental analyzer. Thermogravimetric analysis (TGA) was conducted on a Du Pont Thermal Analyst 2100 system with a TGA 2950 thermogravimetric analyzer at a heating rate of 10 °C/min under nitrogen. Melting points were determined with a Buchi SMP-20 capillary melting point apparatus. Viscosity measurements were proceeded by 10% weight of polymer solutions (in NMP) in contrast to that proceeded by monomer solutions under the same condi-

* Author for correspondence. Telephone: 8863−5712121 ext. 55305. Fax: 8863−5724727. E-mail: linhc@cc.nctu.edu.tw.
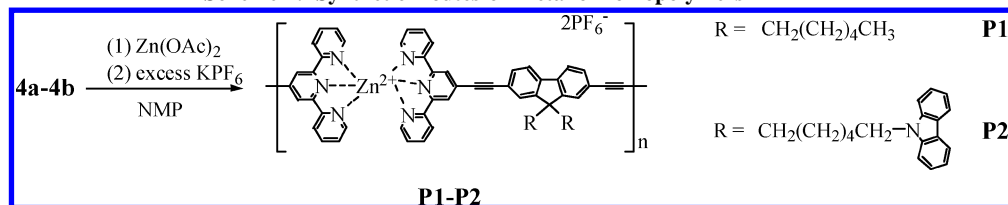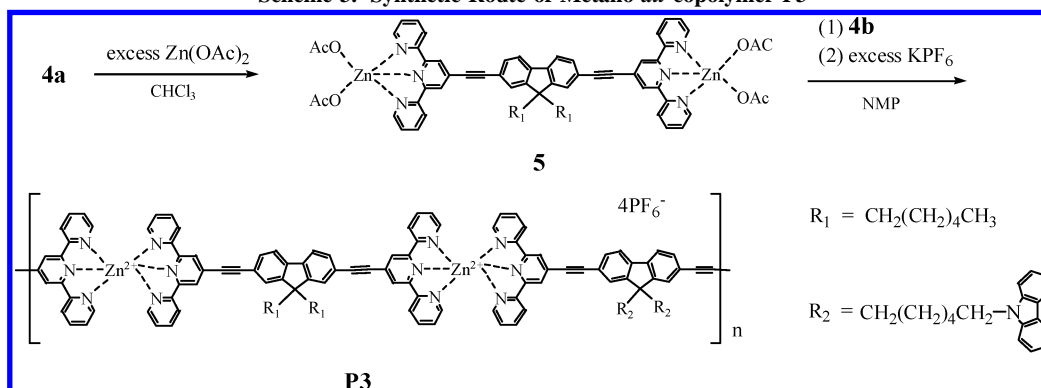† Department of Materials Science and Engineering, National Chiao Tung University.
‡ Institute of Chemistry, Academia Sinica.

Scheme 1. Synthetic Routes of Monomers 4a and 4b
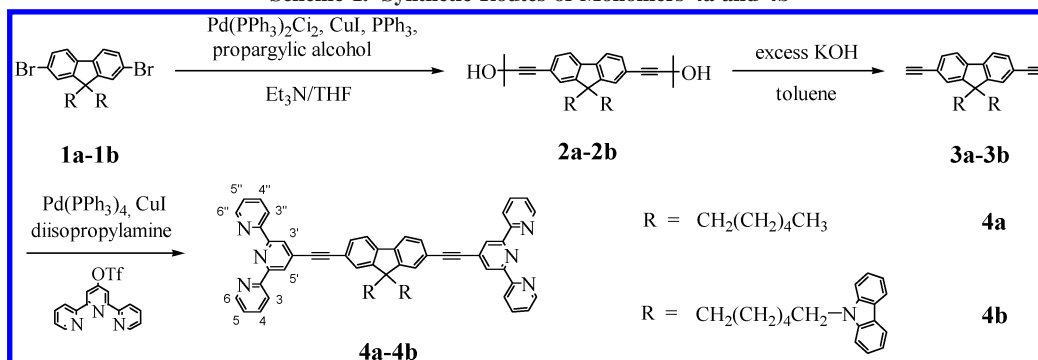
Scheme 2. Synthetic Routes of Metallo-Homopolymers P1−P2

Scheme 3. Synthetic Route of Metallo-*alt*-copolymer P3

tion (with viscosity $\eta = 6$ cP) on a BROOKFILEL DV-III+ RHEOMETER system at 25 °C (100 rpm, spindle number 4). UV−visible (UV−vis) absorption spectra were recorded in dilute DMF solutions (10^{-5} M) on a HP G1103A spectrophotometer, and fluorescence spectra were obtained on a Hitachi F-4500 spectrophotometer. Fluorescence quantum yields were determined by comparing the integrated photoluminescence (PL) density of coumarin-1 in ethanol with a known quantum yield (ca. 5×10^{-6} M, quantum yield = 0.73). Cyclic voltammetry (CV) was performed at a scanning rate of 100 mV/s on a BAS 100 B/W electrochemical analyzer, which was equipped with a three-electrode cell. Pt wire was used as a counter electrode, and an Ag/AgCl was used as a reference electrode in the CV measurements. The CV experiments were performed by solid samples immersed into electrochemical cell containing a 0.1 M tetrabutylammonium hexafluorophosphate (Bu_4NPF_6) solutions (in DMF) at a scanning rate of 100 mV/s at room temperature under nitrogen. Polymer thin solid films were spin-coated on quartz substrates from DMF solutions with a concentration of 10 mg/mL. UV−vis and PL titration were preformed by that 1.0×10^{-5} M of monomer solutions in the solvent of $CH_3CN/CHCl_3$ (2/8 in vol.) was titrated with 50 μl aliquots of a 3.9×10^{-4} M of $Zn(OAc)_2$ solutions in the same solvent composition as described. The addition was done stepwisely and the formation of Zn(II)-coordination polymers was monitored by UV−vis spectroscopy. A series of EL devices with the configuration of ITO/PEDOT: PPS/polymer/BCP(2,9-dimethyl-4,7-diphenyl-1,10-phenanthroline)/Alq₃(tris(8-hydroxyquinoline)aluminum)/LiF/Al were made, where BCP (i.e., 2,9-dimethyl-4,7-diphenyl-1,10-phenanthroline) or Alq₃ (i.e., tris(8-hydroxyquinoline)aluminum) was used as an electron transporting layer.

The ITO substrates were routinely cleaned by ultrasonic treatments in detergent solutions and diluted water, followed by rinsing with acetone and then ethanol. After drying, the ITO substrates were kept in oxygen plasma for 4 min before being loaded into the vacuum chamber. The solutions (10 mg/mL) of light-emitting materials in DMF were spin-coated on glass slides precoated with indium tin oxide (ITO) having a sheet resistance of $\sim$20 Ω/square and an effective individual device area of 3.14 mm². The spin-coating rate was 6000 rpm for 60 s with PEDOT: PPS, 4000 rpm for 60 s with resulting polymers, and the thicknesses of PEDOT: PPS and polymers were measured by an Alfa Step 500 Surface Profiler (Tencor). BCP and Alq₃ were thermally deposited at a rate of 1−2 Å/s under a pressure of $\sim$2 × 10^{-5} Torr in an Ulvac Cryogenic deposition system. Under the same deposition systems and conditions, one layer of LiF was thermally deposited as a cathode at a rate of 0.1−0.2 Å/s, which was followed by capping with an aluminum layer.

Materials. Chemicals and solvents were reagent grades and purchased from Aldrich, ACROS, TCI, and Lancaster Chemical Co. Solvents were purified and dried according to standard procedures. Chromatography was performed with Merck silica gel (mesh 70−230) and basic aluminum oxide, which was deactivated with 4 wt % of water. 4′-[[(Trifuroromethyl)sulfonyl]oxy]-2,2′:6′,6″-terpyridines and compounds **1a** and **1b** were prepared and purified according to literature procedures.[12a−c] The synthetic routes of monomers and metallo-polymers are illustrated in Schemes 1−3.

Syntheses of Monomers. Compound 2a. To a solution of compound **1a** (13.8 g, 28 mmol) in 60 mL of THF/Et₃N (1/1), 3-methyl-1-butyn-3-ol (8.83 mL, 84 mmol) was added. After the solution was degassed with nitrogen for 30 min, Pd(PPh₃)₂Cl₂ (0.19

g, 0.28 mol), PPh$_3$ (2.9 g, 11 mol), and CuI (0.53 g, 2.8 mmol) were added. The reaction was then refluxed at 70 °C under N$_2$ for 12 h. The solvent was removed under reduced pressure. The resulting solid was extracted with CH$_2$Cl$_2$/H$_2$O then dried over MgSO$_4$. The crude product was purified by column chromatography (silica gel, hexane/ethyl acetate = 4/1 in volume) to afford a white solid: mp 96−97 °C. ^{1}H NMR (300 MHz, CDCl$_3$): δ 7.59 (d, *J* = 8.4 Hz, 2H), 7.37−7.41 (m, 4H), 2.09 (s, 2H), 1.88−1.93 (m, 4H), 1.65 (s, 12H), 1.09 (br, 16H), 0.75−0.80 (m, 6H). Yield: 82%. FABMS: *m/e* 498; C$_{35}$H$_{46}$O$_2$ requires *m/e* 498.35.

Compound 2b. The procedure is analogous to that described for **2a** to afford a white solid: mp 101−102 °C. ^{1}H NMR (300 MHz, CDCl$_3$): δ 8.06 (d, *J* = 6.9 Hz, 4H), 7.57 (d, *J* = 7.8 Hz, 2H), 7.30−7.45 (m, 8H), 7.17−7.30 (m, 8H), 4.15 (t, *J* = 6.9 Hz, 4H), 2.04 (s, 2H), 1.95−1.98 (m, 4H), 1.82−1.84 (m, 4H), 1.66 (s, 12H), 1.07 (br, 12H). Yield: 78%. FABMS: *m/e* 817; C$_{58}$H$_{60}$N$_2$O$_2$ requires *m/e* 816.47.

Compound 3a. A mixture of **2a** (0.82 g, 1.63 mmol) and KOH (365 mg, 6.5 mmol) in 60 mL of 2-propanol was heated reflux under N$_2$ with a vigorous stirring for 3 h. The solvent was then removed and crude product was purified by column chromatography (silica gel, hexane) to afford a white solid: mp 154−155 °C. ^{1}H NMR (300 MHz, CDCl$_3$): δ 7.63 (d, *J* = 8.4 Hz, 2H), 7.47−7.49 (m, 4H), 3.17 (s, 2H), 1.87−1.92 (m, 4H), 1.07 (br, 16H), 0.75−0.83 (m, 6H).Yield: 83%. FABMS: *m/e* 382; C$_{29}$H$_{34}$ requires *m/e* 382.27.

Compound 3b. The procedure is analogous to that described for **3a** to afford a white solid: mp 164−165 °C. ^{1}H NMR (300 MHz, CDCl$_3$): δ 8.05 (d, *J* = 6.6 Hz, 4H), 7.87 (d, *J* = 7.8 Hz, 2H), 7.37−7.47 (m, 8H), 7.15−7.30 (m, 8H), 4.15 (t, *J* = 6.3 Hz, 4H), 3.14 (s, 2H), 1.90−1.94 (m, 4H), 1.80−1.84 (m, 4H), 1.05 (br, 12H). Yield: 80%. FABMS: *m/e* 700; C$_{52}$H$_{48}$N$_2$ requires *m/e* 700.38.

Monomer 4a. Compound **3a** (250 mg, 0.5 mmol) and 4′-[[(trifuroromethyl)sulfonyl]oxy]-2,2′:6′,6″-terpyidine (420 g, 1.1 mmol) were dissolved in nitrogen-degassed benzene, then [Pd^0(PPh$_3$)$_4$] (70 mg, 0.06 mmol) was added and followed by nitrogen-degassed ^{i}Pr$_2$NH. The solution was then heated to 70 °C. After complete consumption of starting materials, the solvent was evaporated and the product was purified by column chromatography (alumina, hexane/dichloromethane = 10/1 in vol.) to afford a white solid: mp 206−207 °C. ^{1}H NMR (300 MHz, CDCl$_3$): δ 8.74 (d, *J* = 4.8 Hz, 4H), 8.62−8.66 (m, 8H), 7.89 (t, *J* = 8.1 Hz, 4H), 7.74 (d, *J* = 8.4 Hz, 2H), 7.57−7.59 (m, 4H), 7.34−7.39 (m, 4H), 2.04 (br, 4H), 1.11 (br, 16H), 0.84 (br, 6H). Yield: 77%. FABMS: *m/e* 845; C$_{59}$H$_{52}$N$_6$ requires *m/e* 844.43. Anal. Calcd for C$_{59}$H$_{52}$N$_6$: C, 83.85; H, 6.20; N, 9.94. Found: C, 84.12; H, 6.34; N, 9.63.

Monomer 4b. The procedure is analogous to that described for **4a** to afford a white solid: mp 223−224 °C. ^{1}H NMR (300 MHz, CDCl$_3$): δ 8.74 (d, *J* = 4.8 Hz, 4H), 8.63−8.67 (m, 8H), 8.04 (d, *J* = 7.8 Hz, 4H), 7.88 (t, *J* = 8.4 Hz, 4H), 7.71 (d, *J* = 7.8 Hz, 2H), 7.54−7.58 (m, 4H), 7.30−7.56 (m, 12H), 7.16 (t, *J* = 6.9 Hz, 4H), 4.19 (t, *J* = 7.2 Hz, 4H), 2.01 (br, 4H), 1.70 (br, 4H), 1.18 (br, 12H). Yield: 79%. FABMS: *m/e* 1175; C$_{83}$H$_{66}$N$_8$ requires *m/e* 1174.54. Anal. Calcd for C$_{83}$H$_{66}$N$_8$: C, 84.81; H, 5.66; N, 9.53. Found: C, 85.12; H, 5.89; N, 9.67.

Synthetic Procedures of Metallo-Polymers. Metallo-Homopolymer P1. To monomer **4a** (0.52 mmol) in 30 mL of NMP solution, zinc acetate (0.52 mmol) in NMP (10 mL) was added dropwisely. The resulting solution was heated at 105 °C under a nitrogen atmosphere. After the recaction was stirred for 24 h, excess KPF$_6$ was added into the hot solution. The resulting solution was poured into methanol and the precipitate obtained was purified by repeated precipitations using NMP and ether. The polymers were dried under vacuum at 60 °C for 24 h and collected as yellow solids. Yields: 82%.

Metallo-Homopolymer P2. The procedure is analogous to that described for **P1.** Yields: 80−84%.

Metallo-*alt*-copolymer P3. To zinc acetate (1.25 mmol) in 20 mL of NMP (*N*-methylpyrrolidinone) solution, monomer **4a** (0.61 mmol) in NMP (20 mL) was added dropwisely. After the reaction was stirred at room temperature for 2 h, then monomer **4b** (0.64 mmol) was also added dropwise. The resulting solution was heated to 105 °C under a nitrogen atmosphere. After this was stirred for 24 h, excess KPF$_6$ was added into the hot solution. The resulting solution was poured into methanol, and the precipitate obtained was purified by repeated precipitations using NMP and ether. The polymers were dried under vacuum at 80 °C for 24 h and collected as yellow solids. Yields: 79%.

Results and Discussion

Synthesis and Characterization. The synthetic routes of monomers **4a** and **4b** and a series of metallo-polymers **P1**−**P3** are illustrated in Schemes 1−3. According to Scheme 1, monomers **4a** (with alkyl pendants) and **4b** (with carbazole pendants) were synthesized from compounds **1a** and **1b** reacted with propargylic alcohol via the Sonogashira coupling reaction, and further deprotected by refluxing 2-propanol in a basic condition. Then, a cross-coupling reaction between **3a** and **3b** and 4′-[[(trifluoromethyl)sulfonyl]-oxy]-2,2′:6′,2″-terpyridine in the presence of a catalytic amount of Pd(0) complexes under a basic condition to obtain monomers **4a** and **4b**.[12d] Metallo-homopolymers **P1** and **P2** (see Scheme 2) were obtained by refluxing monomers **4a** and **4b** with zinc acetate at the ratio of 1:1, respectively, in NMP solutions and followed by subsequent anion exchanges, where Zn(II) species from Zn(OAc)$_2$ were used to prepare for the terpyridyl Zn(II))-based metallo-polymers.[11] The key steps in the functionalized two terpyridyl units of monomer **4a** with zinc acetate at the ratio of 1:2 to afford complex **5**. Then, complex **5** as an initiator was coordinated with monomer **4b** at the ratio of 1:1 (as a sequential-coupling method) to obtain metallo-*alt*-copolymer **P3**.

^{1}H NMR Analyses. ^{1}H NMR spectra of monomers **4a** and **4b**, complex **5**, and polymers **P1**−**P3** were recorded in DMSO-d_6 as show in Figure 1. Monomers **4a** and **4b** reveal well-defined ^{1}H peaks for terpyridyl units. Compared with ^{1}H peaks in monomer **4a**, those in terpyridyl units of complex **5** show downfield shifts for (6,6″),(5,5″),(4,4″),(3′,5′),(3,3″)-H. Furthermore, (4,4″)-H in terpyridyl units of complex **5** overlap with the ^{1}H peak of fluorine unit. All polymers exhibited broadening effect and dramatic shifts in ^{1}H peaks of terpyridyl units after coordinating with Zn^{2+} ions.[10−11a] The formation of homopolymers **P1** and **P2** is clearly indicated by the appearance of new sets of ^{1}H peaks and the absence of the original ^{1}H peaks in terpyridyl units, which belong to uncomplexed monomers **4a** and **4b**. The assignment of ^{1}H peaks of terpyridyl units in polymer structures are made by asterisks according to 4-chloro-terpyridine Zn^{2+} complex. In terms of ^{1}H peaks for carbazole pendants, there is no obvious change in chemical shifts between monomer **4b** and polymers **P2** and **P3**. Therefore, the most upshifted ^{1}H peaks in terpyridyl units of polymers **P2** and **P3** could be hidden under the ^{1}H peaks of carbazole pendants. To distinguish the molecular structures between metallo-homopolymer and metallo-*alt*-copolymer, the integrated ratios of the most downfield-shifted ^{1}H peaks in terpyridyl units (*A for **P2** and *A′ for **P3**) and the ^{1}H peaks of pendant alkyl chains (spacer −CH$_2$−) attached to carbazole units (B for **P2** and B′ for **P3**) of polymers **P2** and **P3** were compared. It reveals that the integrated ratio of *A/B is 0.5 for homopolymer **P2** and that of *A′/B′ is 1 for *alt*-copolymer **P3**, which suggests that the integrated ratios of polymers were consistent with the monomer amounts containing pendent carbazole units. According to these results, the amounts of ligand blocks (i.e., **P1** and **P2**: one-block ligands; **P3**: diblock ligands) can be confirmed.[13]

Thermal, Electrochemical, and Viscosity Properties. The thermal, electrochemical, and viscosity properties of polymers
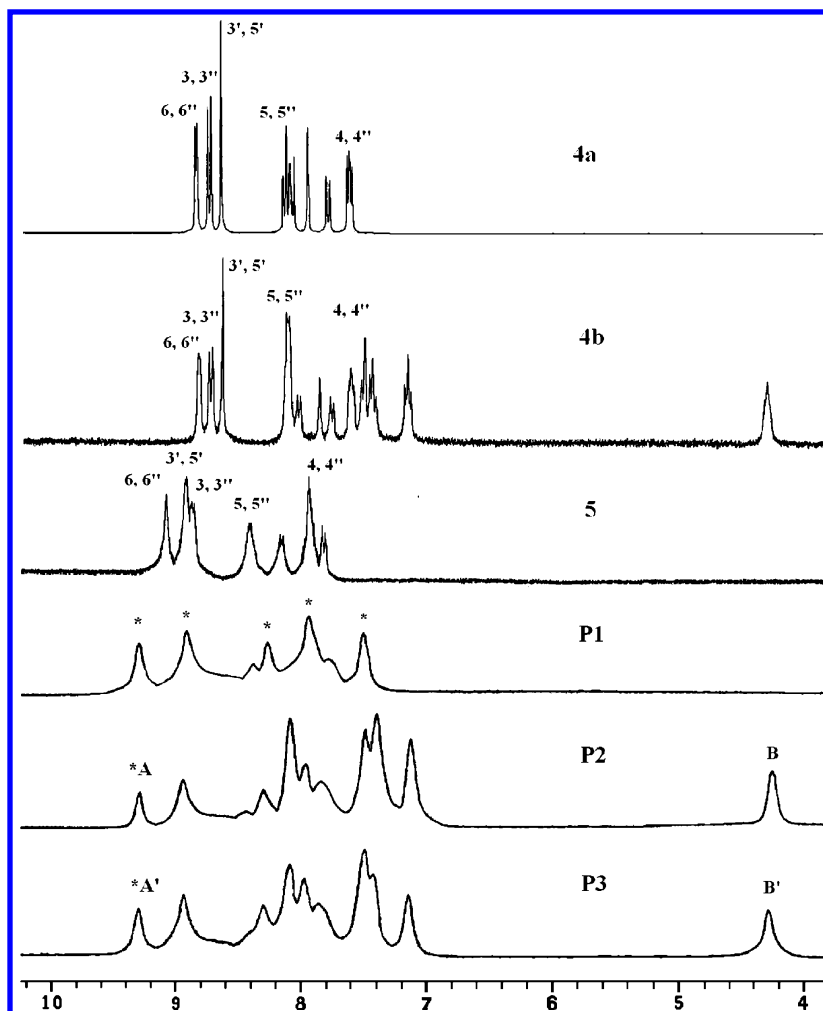
Figure 1. ^{1}H NMR spectra of monomers **4a** and **4b**, complex **5**, and polymers **P1**−**P3** in DMSO-d_6.

Table 1. Physical Properties of Polymers (P1−P3)

polymers	η (cp)[a]	T_d (°C)[b]	E^{red}/peak (V)[c]	E^{LUMO} (eV)[d]	band gap (eV)[e]
P1	9	422	−1.58 (r)	−2.89	3.15
P2	10	399	−1.53 (r)	−2.85	3.14
P3	10	368	−1.55 (r)	−2.88	3.15

[a] Solutions of monomers **4a** and **4b** (10% in weight) in NMP (with viscosity $\eta = 6$ cP, 25 °C) were used as references for determination the viscosity of polymers. [b] Decomposition temperatures (T_d) (5% weight loss) were determined by TGA with a heating rate of 20 °C min^{-1} under N$_2$ atmosphere. [c] Reduction peak in N$_2$-purged DMF, r in parentheses means reversible. [d] LUMO energy level was calculated from the measured reduction potential vs ferrocene/ferrocenium couple in DMF. [e] Optical band gaps were estimated from the absorption spectra in solutions by extrapolating the tails of the lower energy peaks.

P1−**P3** studied by TGA, CV and rheometry, respectively, are summarized in Table 1.

As shown in Figure 2, the decomposition temperatures (T_d) (5% weight loss measured by TGA) of metal precursor Zn(OAc)$_2$, monomers, and polymers under nitrogen were in the range of 210, 345−351, and 368−422 °C, respectively. Both of the monomers and polymers showed the same appearance of two degradation temperatures. In contrast to metal precursor Zn(OAc)$_2$ and monomers, polymers exhibited slightly enhanced thermal stability due to the increased rigidity of the main-chain structures.[11b,c] As the alkyl pendants are attached to polymer backbones, it leads to reduced rigidity of the polymers.[4d,11c] Hence, polymers **P2** and **P3** containing bulky carbazole pendants, which further reduce the π−π stacking of the main-

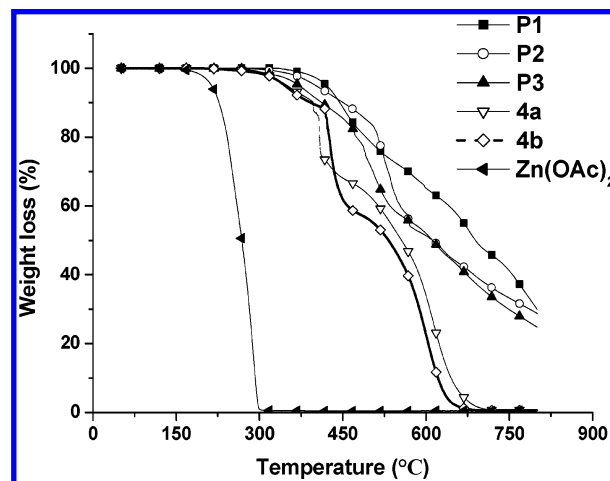**Figure 2.** TGA thermograms of monomers **4a** and **4b**, Zn(OAc)$_2$, and polymers **P1**−**P3** upon heating to 800 °C under nitrogen.

chain structures, show lower T_d values than polymer **P1**. However, polymer **P3** reveals the lowest T_d value, which may be caused by the reduced interchain interaction from the alternating copolymer structure and thus to decrease the rigidity of polymer **P3**. In contrast to metal precursor Zn(OAc)$_2$ and monomers, only polymers possessed 25−30% residual materials upon heating to 800 °C, and similar results of residual ratio in coordination polymers were reported in the literature.[11a] This result suggests that the residual materials are originated from the aggregation of polymers **P1**−**P3** due to π−π stacking of
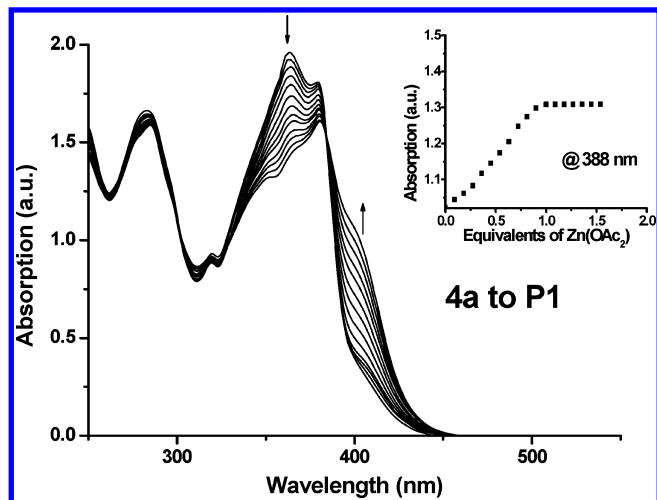
Figure 3. UV−vis spectra acquired (in the process of **4a** to **P1**) upon the titration of monomer **4a** in CH$_3$CN/CHCl$_3$ (2/8 in vol.) with Zn(OAc)$_2$. The spectra are shown at selected Zn^{2+}:**4a** ratios ranging from 0 to 1. The inset shows the normalized absorption at 388 nm as a function of Zn^{2+}:**4a** ratio.

Figure 4. UV−vis spectra acquired (in the process of **4a** to **5**) upon the titration of monomer **4a** in CH$_3$CN/CHCl$_3$ (2/8 in vol.) with Zn(OAc)$_2$. The spectra are shown at selected Zn^{2+}:**4a** ratios ranging from 1 to 2. The inset shows the normalized absorption at 274 nm as a function of Zn^{2+}:**4a** ratio.

Figure 5. UV−vis spectra acquired (in the process of **4b** to **P2**) upon the titration of monomer **4b** in CH$_3$CN/CHCl$_3$ (2/8 in volume) with Zn(OAc)$_2$. The spectra are shown at selected Zn^{2+}:**4b** ratios ranging from 0 to 1. The inset shows the normalized absorption at 425 nm as a function of Zn^{2+}:**4b** ratio.

the fully conjugated main-chain structures. Overall, the combination of metals and ligands in the main-chain coordination polymers can enhance the thermal stability.

All polymers exhibited reversible reduction peaksat around −1.54 V in cathodic scans up to −2.5 V. These peaks are attributed to the reduction of terpyridyl-based moieties.[11,12d] The reduction potentials of these polymers are quite similar to Che's report.[11] The oxidation peaks in the anodic scans up to 1 V of these polymers were absent, because metal oxidation is extremely difficult to be observed for the d^{10} zinc (?) ion species.[15,16] The lowest unoccupied molecular level (LUMO) energy levels were estimated from reduction potentials by the reference energy level of ferrocene (4.8 eV below the vacuum level) according to the following equation:[14] $E^{LUMO} = [−(E^{onset} − 0.45) − 4.8]$ eV. However, the oxidation potentials of all polymers were not detectable, so the highest occupied molecular level (HOMO) energy levels can be estimated by adding LUMO energy levels and optical band gaps. The optical band gaps were estimated from absorption spectra in DMF solution by extrapolating the tails of the lowest energy peaks. The optical band gaps of these polymers (**P1**−**P3**) were ranged from 3.13 to 3.15 eV.[9c,11] Since polymers **P1**−**P3** possess similar backbone structures, there are no obvious changes in the optical band gaps.

Solutions of monomers **4a** and **4b** (10% weight ratio) in NMP with viscosity η = 6 cP at 25°C were used as references for determination the viscosities of polymers. In comparison with the viscosity values of monomers **4a** and **4b**, polymers **P1**−**P3** exhibit increased viscosity values (viscosity η = 9−10 cP) by adding Zn^{2+} ions, and the relative viscosity of polymers to monomers were in the range of 1.5−1.66. The similar phenomenon was also reported by Gordaninejad et al.[17]

UV—Vis and Photoluminescence Titration. To further characterize homopolymers **P1** and **P2** and complex **5**, UV−vis titration experiments were also carried out to confirm their supramolecular structures. Upon addition of Zn^{2+} to monomer **4a** reaching a ratio of 1:1 (Zn^{2+}:**4a**) as shown in Figure 3, the spectra revealed a shift of three other absorption bands at 357, 364, and 402 nm along with one isosbestic point, which suggests that an equilibrium occurred between a finite number of spectroscopically distinct species. The titration curves (Figure 3, insets) showed a linear increase and a sharp end point at the ratio of 1:1 (Zn^{2+}:**4a**), indicating the formation of metallo-

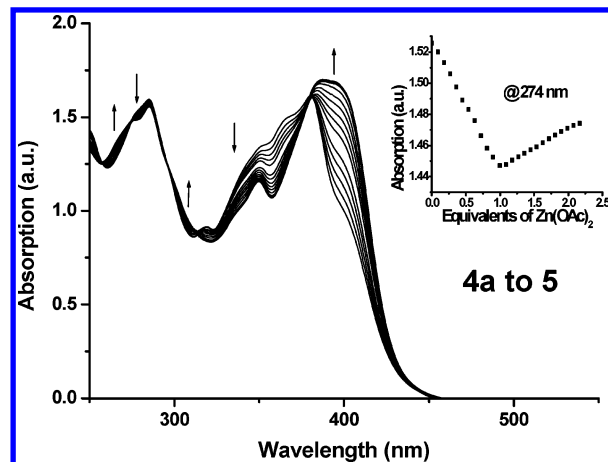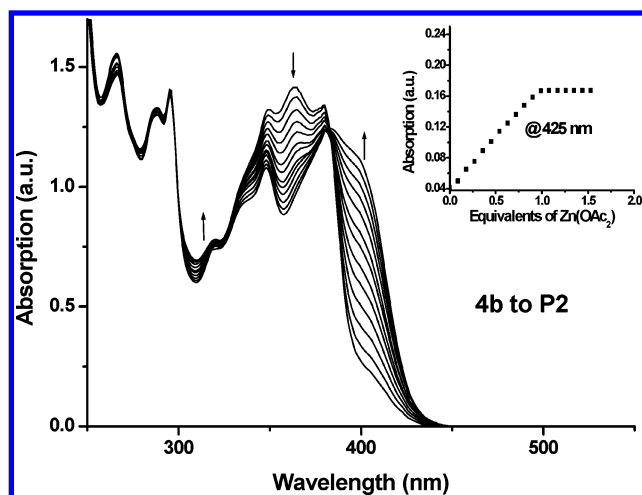polymers. Beyond this point (Figure 4), the subsequent addition of Zn^{2+} induced new peaks at 275, 349, and 388 nm as well as new isosbestic points to form, which points out that another new equilibration arose between a different set of spectroscopically distinct species. Thus, as the ratio of Zn^{2+} to monomer **4a** is above 1:1, depolymerization driven by the formation of chain-terminating complex **5** will occur.[10a,18] Figure 5 depicts that upon addition of Zn^{2+} to monomer **4b** to reach a ratio of 1:1 (Zn^{2+}:**4b**), and the inset spectra also revealed the same results as Figure 3. All polymers displayed a shoulder near the lowest energy absorption (around λ_{Abs} = 400 nm) which corresponds to a charge transfer occurring between the electron-rich central fluorenyl components and the electron-deficient metal-coordinated terpyridyl moieties.[18] The complexation also can be followed by a photoluminescence (PL) titration experiment to further investigate PL properties of homopolymers **P1** and **P2**. In Figure 6, monomer **4a** showed two emission bands around 399 and 418 nm. As the ratio of Zn^{2+}: **4a** reached 1:1, a new emission band at 457 nm was induced. The PL quantum yields of medium complexes (the ratio of Zn^{2+}: **4a** gradually approaching 1:1 in insets of Figure 6) were marginally enhanced and followed by increasing the molar ratio of Zn^{2+} ions.

Table 2. Photophysical Properties of Polymers (P1−P3)

polymer	$\lambda_{Abs,sol}$ (nm)[a]	$\lambda_{max,PL,sol}/\Phi_{PL,sol}$ (nm)[a,b,c]	$\lambda_{Abs,film}$ (nm)	$\lambda_{max,PL,film}$ (nm)
P1	285, 319, 365, 376	418/0.23	289, 338, 353, 400	513
P2	288, 293, 320, 348, 362, 377	420/0.11	289, 295, 335, 399	457 (547)
P3	286, 293, 319, 362, 376	418/0.18	289, 298, 337, 399	459 (527)

[a] Concentration of 1×10^{-6} M in DMF. [b] Coumarin-1 in ethanol (ca. 5×10^{-6} M, quantum yield = 0.73) used as a reference for determination the quantum yields of PL in solutions. The PL quantum yields (in solutions) of monomers 4a and 4b are 0.20 and 0.25, respectively. [c] PL emission shoulders are shown in parentheses.
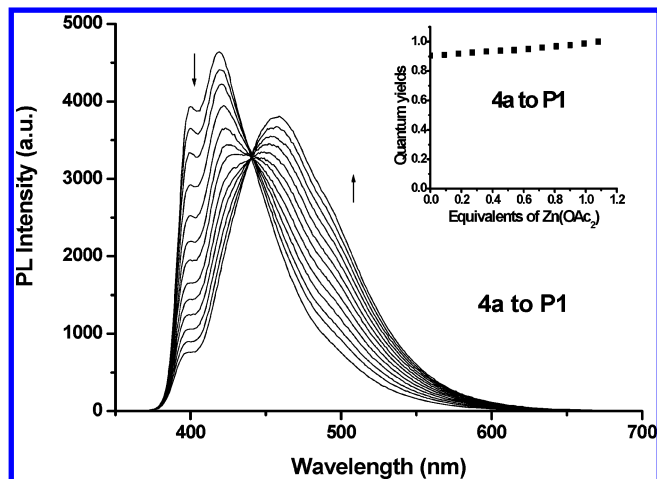

Figure 6. PL spectra acquired (in the process of 4a to P1) upon the titration of monomer 4a in CH$_3$CN/CHCl$_3$ (2/8 in vol.) with Zn(OAc)$_2$. The spectra are shown at selected Zn^{2+}:4a ratios ranging from 0 to 1. The inset shows the quantum yields as a function of Zn^{2+}:4a ratio.
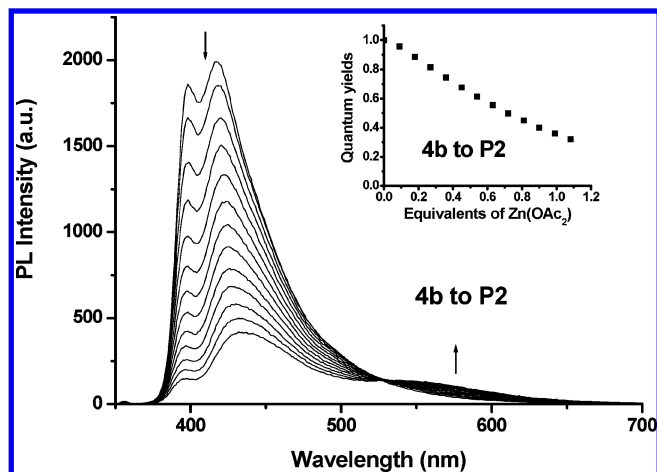

Figure 7. PL spectra acquired (in the process of 4b to P2) upon the titration of monomer 4b in CH$_3$CN/CHCl$_3$ (2/8 in vol.) with Zn(OAc)$_2$. The spectra are shown at selected Zn^{2+}:4b ratios ranging from 0 to 1. The inset shows the quantum yields as a function of Zn^{2+}:4b ratio.

Monomer 4b also showed the same emission band as 4a (shown in Figure 7). As an end point of titration was reached, polymer P2 displayed a significant decrease in PL quantum yield of medium complexes (the ratio of Zn^{2+}: 4b gradually approaching 1:1 in the insets in Figure 7) and a new weak emission band was observed at 558 nm. Because of different pendent groups attached to monomer ligands 4a (with alkyl pendants) and 4b (with carbazole pendants), metallo-polymer P1 exhibited a little higher PL quantum yield than its corresponding monomer 4a, but metallo-polymer P2 displayed a much lower PL quantum yield than its corresponding monomer 4b. Therefore, the PL quantum yields of metallo-polymers can be sufficiently controlled by attaching different pendent groups to monomer ligands.
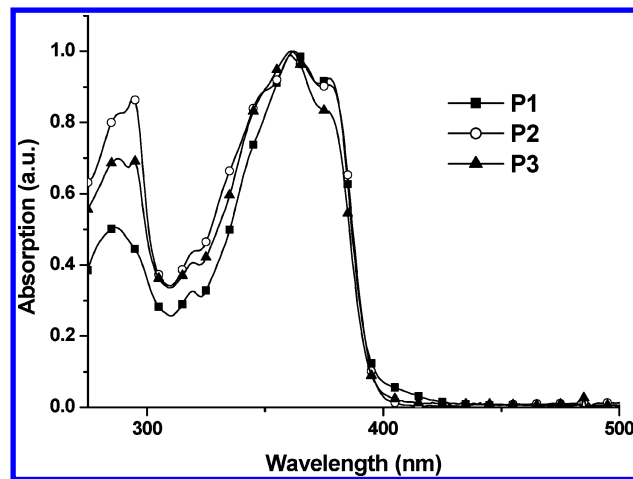

Figure 8. UV−vis spectra of metallo-polymers P1−P3 in DMF solutions.

Photophysical Properties. The photophysical characteristics of polymers P1−P3 were measured by UV−vis absorption and PL spectra in both dilute DMF (N,N-dimethylformamide) solutions and solid films, and their photophysical properties are summarized in Table 2. In Figure 8, similar absorption features were observed in DMF solutions of polymers P1−P3, where the values of λ_{Abs} are around 285, 319, 360, and 378 nm. Interestingly, polymers P2 and P3 showed an additional absorption band at λ_{Abs} = 294 nm, which is associated with carbazole moieties. PL emissions of all polymers are assigned to intraligand ($\pi^*-\pi$) fluorescence. They showed purple-blue colors in DMF solutions, where the values of $\lambda_{max,PL}$ were around 420 nm, and the quantum yields (Φ) were 23%, 11%, and 18% for polymers P1, P2, and P3, respectively (see Table 2). Since polymer P1 (with alkyl pendants) has a higher quantum yield than its monomer 4a (Φ = 0.20) and polymer P2 (with carbazole pendants) has a lower quantum yield than its monomer 4b (Φ = 0.25), it is reasonable to observe that metallo-alt-copolymer P3 has a medium quantum yield value (Φ = 0.18) between P1 (Φ = 0.23) and P2 (Φ = 0.11). These trends fit well to their quantum yield changes of PL titration experiments (as shown in the insets of Figures 6-7). Hence, carbazole pendants are detrimental to the PL quantum yields of metallo-polymers. However, for monomer ligands, 4b with carbazole pendants (Φ = 0.25) has a higher PL quantum yield than 4a with alkyl pendants (Φ = 0.20), so it did not have the same effect on the PL quantum yields of the monomers. Moreover, solid films of these polymers emitted blue to green lights with values of $\lambda_{max,PL}$ ranging at 456−514 nm (Figure 9). From PL emissions of polymer films, polymer P1 showed the largest Stokes shift (ca. 98 nm), which was attributed to the excimer formation resulting from $\pi-\pi$ stacking of aromatic interaction in the solid state.[19,20] On the other hand, both polymers P2 and P3 showed weaker excimer emission bands (around 513 nm) than polymer P1, which indicate that the incorporation of carbazole pedants attached to the C-9 position of fluorene by long alkyl spacers can suppress the excimer formation.
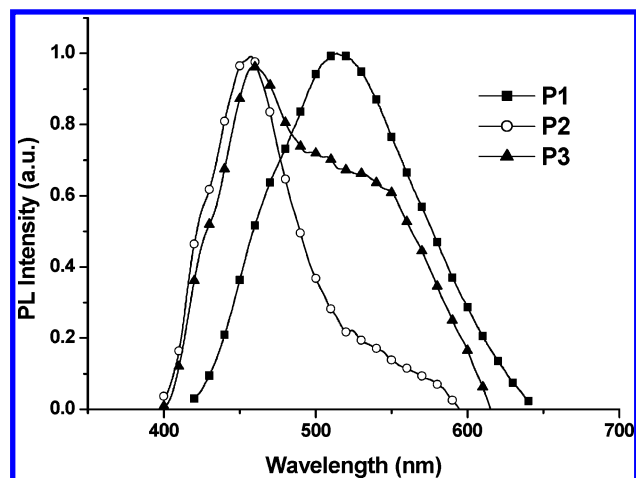
Figure 9. PL spectra of metallo-polymers **P1–P3** in solid films.

Table 3. Electroluminescence (EL) Properties of PLED Devices[a] Containing an Emitting Layer of Polymer (P1–P3)

polymers	$\lambda_{max,EL}$ (nm)	V_{on} (V)[b]	max. luminescence (cd/m²) (V)	power efficiency (cd/A⁻¹)[c]	CIE coordinates (x, y)
P1	551	6.0	1704 (14.5)	0.85	(0.41, 0.52)
P2	549	6.5	2819 (15)	1.11	(0.41, 0.53)
P3	550	6.0	2640 (15)	1.10	(0.41, 0.52)

[a] Device structure: ITO/PEDOT:PSS/polymer(**P1–P3**)/BCP/Alq₃/LiF/Al, where the polymer (**P1–P3**) is an emitting layer. [b] V_{on} is the turn-on voltage. [c] Power efficiencies were obtained at 100 mA/cm².
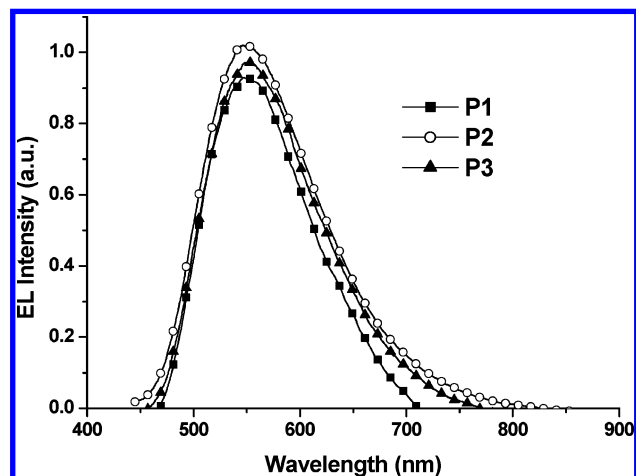

Figure 10. EL spectra of PLED devices with the configuration of ITO/PEDOT:PSS/polymer (**P1–P3**)/BCP/Alq₃/LiF/Al.

Electroluminescence Properties. Polymers **P1–P3** were fabricated into four-layer PLED devices, respectively, with a configuration of ITO/PEDOT:PSS(40–50 nm)/polymer (**P1–P3**) (50–60 nm)/BCP(10 nm)/Alq₃(30 nm)/LiF(1 nm)/Al(150 nm) using standard procedures of spin-coating and vacuum deposition methods, where polymers **P1–P3** were used as the emission layer and PEDOT: PSS as the hole transporter. Besides, either BCP or ALQ was used as an electron transporter.[19c] The EL properties are listed in Table 3. At a bias voltage of 10 V, all PLED devices showed green emissions with $\lambda_{max,EL}$ around 550 (as shown in Figure 10) and its EL intensity was enhanced by increasing the bias voltage. The turn-on voltage of these PLED devices were about 6.0 V, and their maximum efficiencies and luminances were 0.85–1.1 cd A⁻¹ (at 100 mA cm⁻²) and 1704–2640 cd m⁻² (at around 15 V), respectively. Comparing the results of the maximum efficiency and luminance
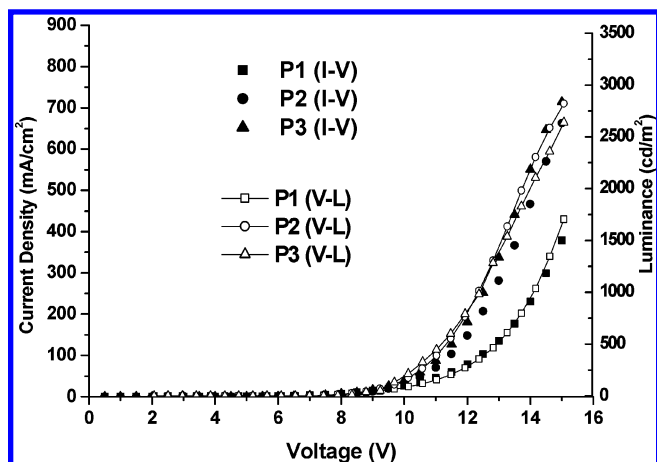

Figure 11. Current–voltage–luminance (I–V-L) characteristics of PLED devices with the configuration of ITO/PEDOT:PSS/polymer (**P1–P3**)/BCP/Alq₃/LiF/Al.

for each device, we can conclude that the incorporation of hole-transporting carbazole units into polymers as pendants will improve the EL performance of the PLED devices.[21,22] It is worthy noting that the EL spectra of these devices did not resemble their corresponding PL spectra in solid films. This is presumably due to the EL and PL emissions originating from different excited states and/or ground states.[11,18a] Figure 11 depicts the current density–voltage–luminance (I–L–V) characteristic curves of polymers **P1–P3**, and similar turn-on voltages for both of the current density and luminance illustrated that a matched balance of both injection and transportation in charges was achieved.[23]

Conclusion

In summary, a logical synthetic protocol for the synthesis of back-to-back bis-terpyridyl-based monomers is presented and novel metallo-supramolecular polymers, including metallo-homopolymers and metallo-*alternating*-copolymer were developed with proper stoichiometric ratios of monomer ligands and ions by self-assembled reactions. Furthermore, the photophysical and electroluminescent properties are greatly affected by the nature of the pendent groups of the coordination polymers. The incorporation of carbazole pendants into polymer side chains reveals that the formation of excimers was suppressed and both PL and EL properties were enhanced. With finely tuned structures incorporating with coordination chemistry, metallo-polymers can provide a new entry to the development of polymeric materials for PLEDs.

References and Notes

(1) (a) Lehn, J. M. *Angew. Chem.* **1988**, *100*, 91; *Angew. Chem., Int. Ed.* **1988**, *27*, 89. (b) Lehn, J. M. *Supramolecular Chemistry, Concepts and Perspective*; VCH: Weinheim, Germany, 1995. (c) Blau, F. *Ber. Dtch. Chem. Ges.* **1888**, *21*, 1077. (d) Kalyanasundaram, K. *Coord. Chem. Rev.* **1982**, *46*, 159.

(2) (a) Morgan, S. G.; Burstall, F. H. *J. Chem. Soc.* **1931**, 20. (b) Morgan, S. G.; Burstall, F. H. *J. Chem. Soc.* **1937**, 1649. (c) Constable, E. C.

Adv. Inorg. Chem. Radiochem. **1986**, *30*, 69. (d) Newkome, G. R.; He, E.; Moorefield, C. N. *Chem. Rev.* **1999**, *99*, 1689.

(3) (a) Wong, C. T.; Chan, W. K. *Adv. Mater.* **1999**, *11*, 455. (b) Antonietti, M.; Lohmann, S.; Eisenbach, C. D.; Schubert, U. S. *Macrol. Rapid. Commun.* **1995**, *16*, 283. (c) Yu, S. C.; Gong, X.; Chan. W. K. *Macromolecules* **1998**, *31*, 5639.

(4) (a) Kelch, S.; Rehahn, M. *Macromolecules* **1997**, *30*, 6185. (b) Schubert, U. S.; Eschbaumer, C. *Angew. Chem., Int. Ed.* **2002**, *41*, 2892. (c) Andres, P. R.; Schubert, U. S. *Adv. Mater.* **2004**, *16*, 1043. (d) Knapton, D.; Iyer, P. K.; Rowan, S. J.; Weder, C. *Macromolecules* **2006**, *31*, 5639.

(5) (a) Dobrwa, R.; Würthner, F. *J. Polym. Sci., Part A: Polym. Chem.* **2005.** 43. 4981. (b) Hofmier, H.; Schubert, U. S. *Chem. Commun.* **2005**, 2423.

(6) (a) Archer, R. D. *Coord. Chem. Rev.* **1993**, *93*, 49. (b) Rehahn, M. *Acta Polym.* **1998**, *49*, 201. (c) Manners, I. *Science* **2001**, *294*, 1664.

(7) (a) Constable, E. C. *Macromol. Symp.* **1995**, *98*, 503. (b) Constable, E. C.; Cargill Thompson, A. M. W. *J. Chem. Soc., Dalton. Trans.* **1992**, 3467. (c) Schütte, M.; Kurth, D. G.; Linford, M. R.; Cölfin, H.; Möhwald, H. *Angew. Chem., Int. Ed. Engl.* **1998**, *37*, 2891.

(8) (a) Sauvage, J. P.; Collin, J. P.; Chambron, J. C.; Guillerez, S.; Coudret, C.; Balzani, V.; Barigelletti, F.; De, Cola., L.; Flamigni, L. *Chem. Rev.* **1994**, 94, 993. (b) Barigelletti, F.; Flamigni, L. *Chem. Soc. Rev.* **2000**, *29*, 1.

(9) (a) Ng, W. Y.; Gong, X.; Chan. W. K. *Chem. Mater.* **1999**, *11*, 1165. (b) Hofmeier, H.; Schubert, U. S. *Chem. Soc. Rev.* **2004**, *33*, 373. (c) Chu, Q.; Pang, Y. *J. Polym. Sci., Part A: Polym. Chem.* **2006**, *44*, 2338.

(10) (a) Dobrwa, R.; Würthner, F. *Chem. Commun.* **2002**, 319. (b) Dobrwa, R.; Lysetska, M.; Ballester, P.; Grüne, M.; Würthner, F. *Macromolecules* 2005, *38*, 1315. (c) Wang, X. Y.; Guzreo, A. D.; Schmehl, R. H. *Chem. Commun.* **2002**, 2344. (d) Goodall, W.; Williams, J. A. G. *Chem. Commun.* **2001**, 2514.

(11) (a) Yu, C. S.; Kowk, C. C.; Chan, W. K.; Che, C. M. *Adv. Mater.* **2003**, *15*, 1634. (b) Yu, S. C.; Hou, S.; Chan. W. K. *Macromolecules* **2000**, *33*, 3259. (c) Huang, F.; Wu, H.; Wang, D.; Wang, W.; Cao, Y. *Chem. Mater.* **2004**, *16*, 708.

(12) (a) Sung, H. H.; Lin, H. C. *Macromolecules* **2004**, *37*, 7945. (b) Potts, K. T.; Konwar, D. *J. Org. Chem.* **1991**, *56*, 4851. (c) Sung, H. H.; Lin, H. C. *J. Polym. Sci., Part A: Polym. Chem.* **2005**, *43*, 2700. (d) Ziessel, R.; Khatyr, A. *J. Org. Chem.* **2000**, *65*, 3126.

(13) (a) Kelch, S.; Rehahn, M.; *Macromolecules* **1999**, *32*, 5818. (b) Schmelz, O.; Rehahn, M. *e-Polym.* **2002**, no. 047.

(14) Janitetz, S.; Bradley, D. D. C.; Grelly, M.; Giebeler, C.; Inbasekaran, M.; Woo, E. P. *Appl. Phys. Lett.* **1998**, *73*, 2453.

(15) (a) Loiseau, F.; Pietro, C. D.; Serroni, S.; Campagna, S.; Licciardello, A.; Manfredi, A.; Pozzi, G.; Quici, S. *Inorg. Chem.* **2001**, *40*, 4901. (b) Hwang, S. H.; Wang, P.; Moorefield, C. N.; Godinez, L. A.; Manriquez, J.; Bustos, E.; Newkome, G. R. *Chem. Commun.* **2005**, 4672.

(16) (a) Thomas, K. R. J.; Chang, C. P.; Chuen, C. H.; Chenu, C. C.; Lin, J. T. *J. C. C. S.* **2002**, *49*, 833. (b) Newkome, G. R.; Cho, T. J.; Moorefield, C. N.; Cush, R.; Russo, P. S.; Godinez, L. A.; Saunder, M. J.; Mohapatra, P. P. *Chem.—Eur. J.* **2002**, *8*, 2946. (c) Newkome, G. R.; Cho, T. J.; Moorefield, C. N.; Mohapatra, P. P.; Godinez, L. A. *Chem.—Eur. J.* **2004**, *10*, 1493.

(17) Hu, B.; Fuchs, A.; Huseyl, S.; Gordaninejad, F. *J. Appl. Polym. Sci.* **2006**, *100*, 2464.

(18) (a) Iyer, P. K.; Beck, J. B.; Weder, C.; Rowan, S. J. *Chem. Commun.* **2005**, 319. (b) Wang, X. Y.; Guerzo, A. Del; Schmehl, R. H. *Chem. Commun.* **2002**, 2344.

(19) (a) Desiraju, G. R.; Gavezotti, A. *J. Chem. Soc., Chem. Commun.* **1989**, 621. (b) Desiraju, G. R. *Chem. Commun.* **1997**, 1475. (c) Kwok, C. C.; Yu, S. C.; Sham, S. T.; Che, C. M. *Chem. Commun.* **2004**, 2758.

(20) (a) Alcock, N. W.; Barker, P. R.; Haider, J. M.; Hannon, M. J.; Painting, C. L.; Pikramenou, Z.; Plummer, E. A.; Rissanen, K.; Saarenketo, P. *J. Chem. Soc., Dalton Trans.* **2000**, 1447. (b) Ishow, E.; Gourdon, A.; Launay, J. P. *Chem. Commun.* **1998**, 1909.

(21) (a) Lee, Y. Z.; Chen, X.; Chen, S. A.; Wei, P. K.; Fann, W. S. *J. Am. Chem. Soc.* **2001**, *123*, 2296. (b) Wu, F. I.; Reddy, S.; Shu, C. F.; Liu, M. S.; Jen, A. K. Y. *Chem. Mater.* **2003**, *15*, 269.

(22) (a) Burn, P. L.; Grice, A. W. Tajbkhsh, A. Bradley, D. D. C.; Thomas, A. C. *Adv. Mater.* **1997**, *9*, 1171. (b) Jin, Y.; Kim, J. Y.; Park, S. H.; Kim, J.; Lee, S.; Lee. K.; Shu, H. *Polymer* **2005**, *46*, 12158.

(23) (a) Wu, C. W.; Lin, H. C. *Macromolecules* **2006**, *39*, 7232. (b) Shu, C. F.; Dodda, R.; Wu, F. I.; Liu, M. S.; Jen, A. K. Y. *Macromolecules* **2003**, *36*, 6698.